Nucleic Acids Research, 1997, Vol. 25, No. 17 **3421–3427**

Evidence for a hydroxide ion bridging two magnesium ions at the active site of the hammerhead ribozyme

Thomas Hermann, Pascal Auffinger, William G. Scott[1] and Eric Westhof*

Institut de Biologie Moléculaire et Cellulaire du CNRS, 15 rue René Descartes, F-67084 Strasbourg, France and [1]Department of Chemistry, Indiana University, Bloomington, IN, USA

Received May 30, 1997; Revised and Accepted July 10, 1997

ABSTRACT

In the presence of magnesium ions, cleavage by the hammerhead ribozyme RNA at a specific residue leads to 2′3′-cyclic phosphate and 5′-OH extremities. In the cleavage reaction an activated ribose 2′-hydroxyl group attacks its attached 3′-phosphate. Molecular dynamics simulations of the crystal structure of the hammerhead ribozyme, obtained after flash-freezing of crystals under conditions where the ribozyme is active, provide evidence that a μ-bridging OH^- ion is located between two Mg^{2+} ions close to the cleavable phosphate. Constrained simulations show further that a flip from the C3′-*endo* to the C2′-*endo* conformation of the ribose at the cleavable phosphate brings the 2′-hydroxyl in proximity to both the attacked phosphorous atom and the μ-bridging OH^- ion. Thus, the simulations lead to a detailed new insight into the mechanism of hammerhead ribozyme cleavage where a μ-hydroxo bridged magnesium cluster, located on the deep groove side, provides an OH^- ion that is able to activate the 2′-hydroxyl nucleophile after a minor and localized conformational change in the RNA.

INTRODUCTION

The hammerhead ribozyme is a catalytically active RNA that cleaves a phosphodiester bond within its own backbone (1). The hammerhead RNA comprises three stems connected by single-stranded regions that contain conserved bases that are required for ribozyme activity (Fig. 1a) (2). Self-cleavage of the hammerhead RNA depends on divalent cations such as Mg^{2+}. There is evidence (3) that a hydroxide ion bound to a divalent cation abstracts the proton from the cleavage-site 2′-hydroxyl, which then attacks the adjacent 3′-phosphate (Fig. 1b and c) (4,5). A second divalent cation may be necessary for stabilizing the pentacoordinated phosphate transition state or, as was suggested recently (3,6), one metal ion may provide both functions. The positions of five Mg^{2+} ions bound to the hammerhead RNA were determined by X-ray crystallography (Fig. 1a) (6,7). One of the Mg^{2+} (site 6) was found bound to the cleavage-site phosphate in a hammerhead ribozyme captured by flash-freezing crystals after soaking with Mg^{2+} at pH 8.5, conditions under which the ribozyme cleaves in the crystal at room temperature (6). This phosphate-bound Mg^{2+} ion at site 6 is thus considered part of the active site of the ribozyme (6). A second Mg^{2+} (site 1) is located 4.25 Å apart from the site 6 cation (Fig. 1a) (6). In the crystal structure of the hammerhead RNA the cleavage-site 2′-hydroxyl is not in a favourable position for the attack at the adjacent phosphate. A conformational change in the hammerhead RNA during the cleavage reaction was therefore proposed (6–9). However, the nature and extent of the required conformational changes are unknown.

The catalytic mechanism for hammerhead cleavage still contains controversial components (reviewed in 10). Based on several experiments (11,12), a double-metal-ion mechanism has been put forward in which the metal ions bind directly to the attacking 2′-OH and leaving 5′ oxygen, without direct coordination to the *pro*-R_P oxygen of the cleavable phosphate (13, K.Taira, private communication). Our working hypothesis here was to analyze the crystal structure of a catalytic hammerhead intermediate obtained after flash-freezing in presence of Mg^{2+} ions at pH 8.5 (6). The crystal structure shows two Mg^{2+} ions bound in the deep groove with one ion directly bound to the *pro*-R_P oxygen of the cleavable phosphate (Fig. 1d).

We have used molecular dynamics (MD) simulations to investigate the dynamical flexibility of the hammerhead RNA. MD calculations, using an explicit solvent model along with an efficient treatment of the long-ranging electrostatic interactions by the Ewald summation method (14), have recently been demonstrated to be successful for reliable simulations of RNA molecules (15,16). The calculations were done within the AMBER4.1 force field (17) using the previously adjusted and validated parameters (18). It was the aim of this work to examine how dynamically occurring conformational changes in the hammerhead RNA could be integrated into a consistent mechanistic model for hammerhead ribozyme cleavage. We appreciate the fact that the halftime of the cleavage reaction is in the minute timescale, while the MD simulations cover the picosecond range, and we thus do not pretend to simulate the catalytic reaction in real-time. The simulation of a chemical cleavage reaction itself within a complex structural framework such as the hammerhead RNA is not feasible with currently available computational methods. However, it was our aim to demonstrate that careful MD simulations based on the freeze-trapped crystal structure of an active hammerhead ribozyme are helpful for defining pathways

*To whom correspondence should be addressed. Tel: +33 3 8841 7046; Fax: +33 3 8860 2218; Email: westhof@ibmc.u-strasbg.fr

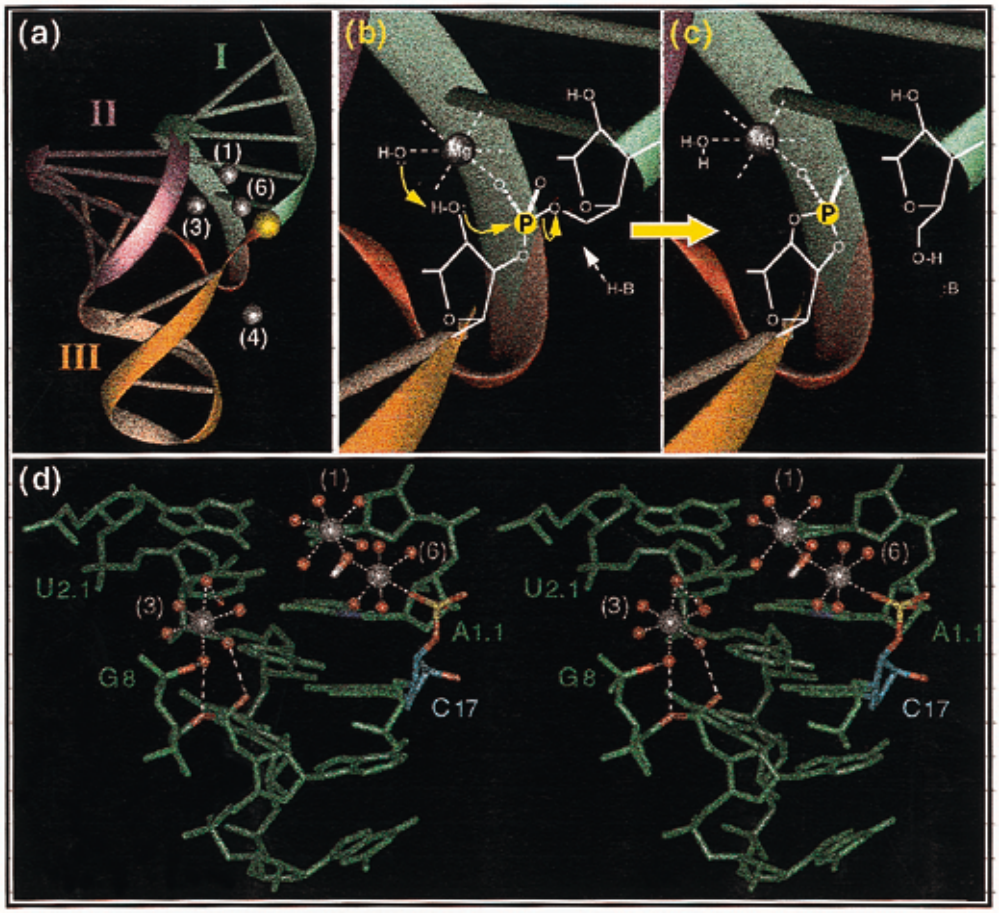

Figure 1. Three-dimensional structure of the hammerhead RNA as determined by crystal structure analysis after flash-freezing at pH 8.5 (6). **(a)** The positions of four Mg^{2+} ions (1, 3, 4, 6) in proximity to the cleavable phosphate (gold) are shown. Two sites were omitted, namely the ion at site 2 in stem II which is 15 Å apart from the active site and site 5 that binds Mn^{2+} but not Mg^{2+} (6). **(b** and **c)** General mechanism previously proposed for hammerhead cleavage (3–5). Hydroxide coordinated to a Mg^{2+} ion that is bound to the cleavable phosphate activates the cleavage-site 2′-hydroxyl group, which then attacks the adjacent 3′-phosphate (b). The cleavage gives rise to a 2′3′-cyclic phosphate and a 5′-hydroxyl end (c). **(d)** Stereoview of a snapshot taken after 400 ps of MD simulation illustrating the hydration pattern of Mg^{2+} ions at sites 1, 3 and 6. Shown are nucleotides $G_{2.2}$–G_8 of the connection between helices I and II and C_{17}–$C_{1.2}$ in the cleavable strand. $Mg^{2+}{}_{(6)}$ is bound to the *pro*-R_P phosphate oxygen of $A_{1.1}$. The μ-bridging OH^- ion is shown in ball-and-stick representation between the two metals. Water molecules in the first coordination sphere around the Mg^{2+} ions are depicted as red spheres. Hydrogen bonds of metal coordinated water molecules stable during the simulations are found to N7 of $A_{1.1}$, to phosphate oxygens of U_7 (*pro*-R_P and O5') and G_8 (*pro*-S_P), and to O4 of $U_{2.1}$. For clarity, the water molecules solvating the system are not shown.

around the equilibrium conformation which could lead towards an activated transition state where the proximity of the reactive groups would allow the cleavage reaction to proceed.

MATERIALS AND METHODS

The AMBER4.1 package (17) was used for MD simulations. RNA atomic coordinates were from a previously published crystal structure analysis of an active hammerhead ribozyme freeze-trapped at pH 8.5 (6). Parameters for Mg^{2+} ions were from Åqvist (19), those for OH^- from Lee *et al.* (20). The RNA was placed in a rectangular box of SPC/E water (21) containing ~6300 solvent molecules. Fifty Na^+ and 18 Cl^- ions, consistent with a concentration of 380 mM Na^+ and 140 mM Cl^-, were placed according to the electrostatic potential around the solute such that no ion was closer than 4.5 Å to any solute atom.

The simulations were run with a time step of 2 fs at a constant temperature of 298 K and a constant pressure of 1 atm. The SHAKE algorithm (22) was used to constrain the X-H bond lengths. Van der Waals interactions were truncated at 9.0 Å, while not cut-off was applied on the electrostatic term. The electrostatic interactions were calculated with the Particle Mesh Ewald method (23) with a charge grid spacing close to 1.0 Å. An elaborate equilibration protocol was refined from protocols used in our preceding work (15,16) to allow for a careful accommodation of the water structure around the RNA and Mg^{2+} ions. Three ps of water equilibration at 298 K with all ions and RNA fixed were followed by a restart at 10 K and heating to 298 K in steps of 50 K with 2 ps at each temperature where water, Na^+ and Cl^- ions were allowed to move. After 10 ps at 298 K a restart at 10 K was performed while the RNA non-hydrogen atoms were constrained with 20 kcal and Mg^{2+} ions with 10 kcal to their positions in the crystal structure. The system was heated to 298 K in steps of 50 K with 5 ps at each temperature. Subsequently the constraint on the Mg^{2+} ions was gradually removed during 40 ps simulation at

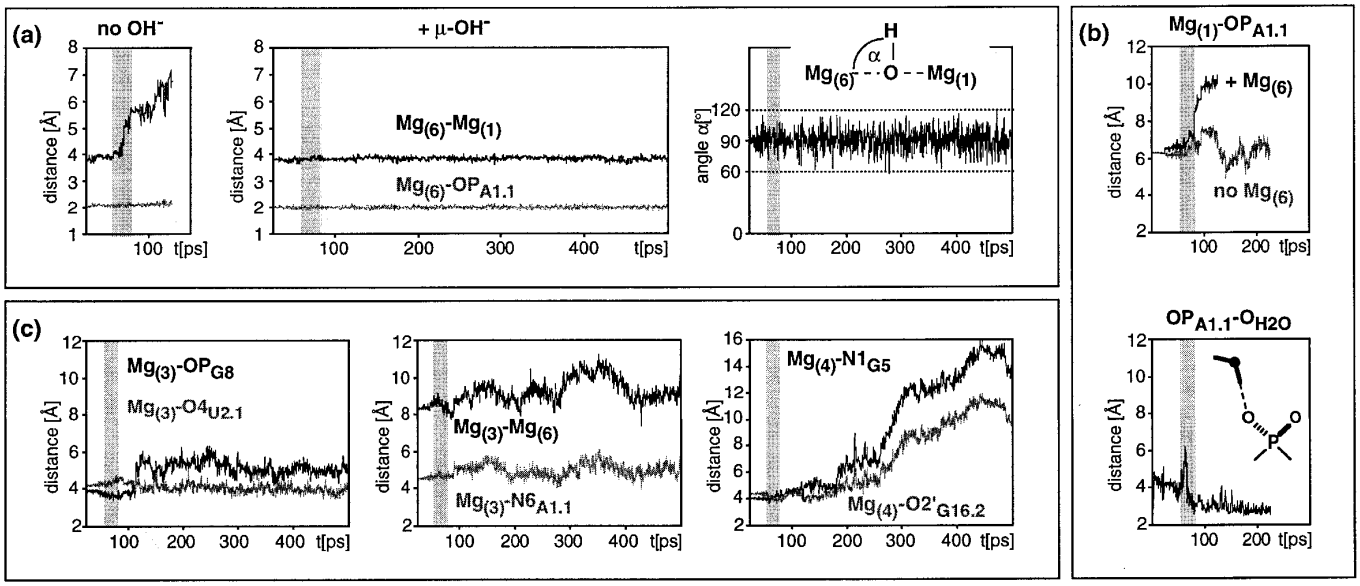

Figure 2. Dynamical behaviour of the Mg^{2+} ions (**a**, **b** and **c**). The simulation phase where the constraints on the Mg^{2+} ions were released is shaded in grey. (**a**) Distances between the Mg^{2+} ions at sites 1 and 6 and between $Mg^{2+}_{(6)}$ and the *pro*-R_P phosphate oxygen of $A_{1.1}$. In the simulation without a μ-bridging OH^- (left) the $Mg^{2+}_{(1)}$ was displaced by 3 Å during the equilibration phase after which the calculation was stopped. Introduction of a μ-bridging OH^- between $Mg^{2+}_{(1)}$ and $Mg^{2+}_{(6)}$ resulted in stabilisation of $Mg^{2+}_{(1)}$ (middle). The stable binding of $Mg^{2+}_{(6)}$ to the phosphate of $A_{1.1}$ is not affected by addition of the μ-OH^-. During the simulation the axis of the μ-OH^- stayed perpendicular to the line connecting $Mg^{2+}_{(1)}$ and $Mg^{2+}_{(6)}$ (right). We observed that the hydrogen atom of the μ-OH^- rotated in the plane perpendicular to this line. (**b**) When the Mg^{2+} ion at site 6 is not present, as in the pH 5.0 crystal structure, the $Mg^{2+}_{(1)}$ ion stayed bound close to its original position as indicated by the plot of the distance between $Mg^{2+}_{(1)}$ and the *pro*-R_P phosphate oxygen of $A_{1.1}$ (top). A water molecule hydrogen-bonded to both the *pro*-R_P phosphate oxygen of $A_{1.1}$ and to a hydration water of $Mg^{2+}_{(1)}$ occupied the crystal structure position of $Mg^{2+}_{(6)}$ during the simulation (bottom). (**c**) Distances between the Mg^{2+} ions at sites 3 and 4 and atoms of the RNA. $Mg^{2+}_{(3)}$ remained stably bound to the RNA (left two panels), while $Mg^{2+}_{(4)}$ dissociated after 200 ps (right). Interactions of $Mg^{2+}_{(3)}$ with the RNA are mediated via water bridges (Fig. 1d). Rearrangement of water bridges between $Mg^{2+}_{(3)}$ and the G_8 phosphate at 120 ps leads to a shifting of the distance between this ion and the *pro*-S_P oxygen of G_8. The resulting hydration pattern remains stable until the end of the simulation. The position of $Mg^{2+}_{(3)}$ relative to the RNA is not affected by this rearrangement as indicated by the distances to three reference atoms [O4 of $U_{2.1}$, N6 of $A_{1.1}$ and $Mg^{2+}_{(6)}$]. O4 of $U_{2.1}$ forms a contact to $Mg^{2+}_{(3)}$ via a water bridge while $A_{1.1}$ is the nucleotide stacking on top of C_{17} both of which are linked by the cleavable phosphate (Fig. 1d).

298 K. Finally, after a restart at 10 K, the system was again heated to 298 K in 5 ps steps of 50 K without applying any constraints.

RESULTS AND DISCUSSION

Evidence for a bridging OH^- ion between two Mg^{2+} ions at the hammerhead active site

We have gathered evidence from MD simulations of the crystallized hammerhead RNA that at least one bridging OH^- is required to stabilize the two Mg^{2+} ions at sites 6 and 1. We performed simulations on the fully hydrated and neutralized hammerhead RNA in presence of the Mg^{2+} ions located at the sites observed in the pH 8.5 crystal structure (Fig. 1a) (6). Special care was taken when equilibrating the system of RNA, ions and solvent. An elaborate heating protocol was employed to ensure relaxation of the RNA and at the same time a favourable arrangement of solvent molecules around both RNA and Mg^{2+}. First, solvent water was allowed to equilibrate, while RNA and ions were fixed followed by a simulation phase where the constraints on the ions and the RNA were successively removed (see Materials and Methods). The quality of the trajectories obtained in our MD calculations is attested by the fact that the hammerhead RNA retained its structural integrity in all simulations. The RMS deviation was in the range of 2.0 Å after 500 ps of calculation. Stems I and II, roughly parallel in the starting crystal structure, tilted towards each other during the simulations. The parallel stem geometry in the crystal is stabilized by the packing of two hammerhead molecules which stack their stem blunt ends against each other leading to a pseudocontinuous helical packing scheme (6). In the crystal structure of a different RNA/DNA hammerhead molecule this contact between stem ends is absent and, consequently, stems I and II are tilted (8). Similarly, in our simulations the absence of crystal contacts lead to tilting of the stems. However, no base-pair breaking was observed in the stem regions.

In a first set of simulations we observed that the Mg^{2+} ion at site 1 was not stable at the position of the crystal structure (Fig. 2a) despite the fact that this ion is the most tightly bound one, as suggested by its appearance in the early electron density maps. When the positional constraints on the Mg^{2+} ions were removed during the equilibration procedure, the cation at site 1 moved rapidly away from its original location in proximity to the Mg^{2+} ion at site 6 while the latter stayed at its original position bound to the phosphate of $A_{1.1}$ (Fig. 2a). The electrostatic repulsion between the two Mg^{2+} ions at sites 1 and 6 apparently destabilized the arrangement found in the crystal structure for these ions.

In order to decrease the repulsion of the Mg^{2+} ions at sites 1 and 6 we introduced a μ-bridging OH^- (Fig. 1d). For positioning the OH^- we replaced a water molecule which, during our first simulation, formed a bridge between the two cations while they were still constrained at their positions in the crystal structure. A similar approach was used by Lee and coworkers for the simulation of a Z-DNA crystal that contained clusters of Mg^{2+} ions (20).

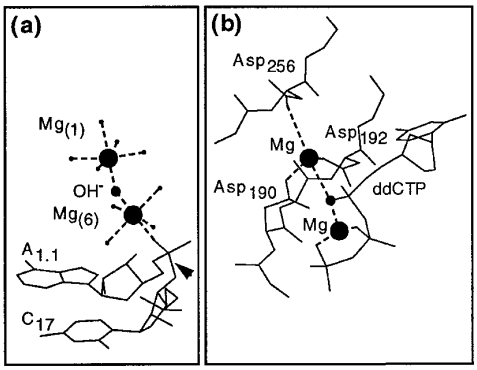

Figure 3. Comparison of the active sites of the hammerhead ribozyme **(a)** and the rat DNA polymerase β **(b)** (after 33). (a) The proposed μ-bridging OH^- ion between the Mg^{2+} ions at sites 6 and 1 (distance 4.3 Å) (6) in the hammerhead RNA is shown as smaller sphere along with water molecules coordinated to the metal ions during MD simulations. The cleavable phosphodiester bond is indicated by an arrow. (b) At the active site of the DNA polymerase β the anionic α-phosphate oxygen (smaller sphere) of the substrate dideoxycytidine triphosphate (ddCTP) is bridging two Mg^{2+} ions (distance 4.6 Å) (33). The position of three metal-coordinated aspartate residues is indicated, which are conserved in the active site of nucleic acid polymerases (41,42).

In the subsequent simulations of the hammerhead RNA the OH^- ion was constrained during the first phase of equilibration as were the Mg^{2+} ions. Yet, after complete removal of the constraints, the complex of the two Mg^{2+} ions at sites 1 and 6 along with the bridging OH^- maintained its geometry over the whole 500 ps simulation period (Fig. 2a). Thus, the OH^- sucessfully moderates the electrostatic repulsion between the two proximate Mg^{2+} ions. In the presence of the bridging OH^- ion, the Mg^{2+} ion at site 1 remained very stable at its crystal structure position in line with the observation that this cation is always seen in X-ray analysis. Despite the fact that site 1 is adjacent to a non-conserved region of the hammerhead RNA, specific binding of cations could be favoured independently of the sequence because this site is located in the deep groove of stem I which displays the lowest electrostatic potential around an RNA helix (24).

The metal ion at site 1 was not stabilized when instead of an OH^- ion either one or two water molecules were placed bridging the Mg^{2+} ions at sites 1 and 6 (data not shown). In all such instances, the repulsion between the two adjacent metal ions rapidly lead to breaking of the water bridges, expelling the Mg^{2+} ion at site 1 from its original position. However, the Mg^{2+} ion at site 1 was not expelled from its original position in simulations where the ion at site 6 was not present (Fig. 2b). This corresponds to the situation observed in crystals of the hammerhead RNA grown at pH 5.0 where a Mg^{2+} ion is bound at site 1 but not at site 6 which is occupied by a water molecule (6). In agreement with this finding, we observe in such simulations a water molecule linking both the *pro*-R_P phosphate oxygen of $A_{1.1}$ and a hydration water of Mg^{2+} ion at site 1 (Fig. 2b).

During the different simulations the Mg^{2+} ion at site 3 stayed bound to the RNA while the ion at site 4 dissociated from the RNA (Fig. 2c). The Mg^{2+} at site 3 stabilizes the turn between helices I and II by interacting with the phosphates of G_8 and U_7 and with the side-chain of $U_{2.1}$ (Fig. 1d). The distance between the Mg^{2+} at site 3 to the ion at site 6, which is bound to the cleavable phosphate, remained in the range found in the crystal structure (8–10 Å) (Fig. 2c). Therefore, it is unlikely that the Mg^{2+} ion at site 3 is directly involved in the chemistry of the cleavage reaction. Following our simulations we have no clues regarding the Mg^{2+} ion at site 4, which is bound to G5, a nucleotide essential for catalysis (2), since this ion dissociated in the present simulations.

Experimental results in line with the proposal of a bridging OH^- ion

While for X-ray crystal structure analysis it is difficult to distinguish between water molecules and hydroxide ions, it is hoped that MD simulations can help to elucidate such details of the solvation structure of metal ions. This could be especially meaningful for the hammerhead RNA where one of the crystallographically identified Mg^{2+} ions is only observed after freeze-trapping at high pH (site 6) (6). In the present MD simulations, the binuclear metal center was not stable, but could be stabilized as a μ-hydroxo-bridged metal complex. Following the prevalent mechanism for catalytic cleavage (6) which involves a metal hydroxide activating the 2′-hydroxyl group for nucleophilic attack and where the reaction rate increases as pH is increased (4), it is tempting to suggest that the μ-hydroxo-bridged metal complex is implicated in the chemistry of the ribozyme catalysis. It was proposed (6) that the Mg^{2+} ion at site 6 provides two basic functions required for ribozyme cleavage. First, by binding of Mg^{2+} close to the cleavable phosphate a conformational change is induced that is required for in-line attack of the active-site 2′-hydroxyl. Second, the same Mg^{2+} carries an OH^- ion that is necessary for the deprotonation at the cleavage-site 2′-hydroxyl in the base-catalyzed step of the cleavage reaction.

The present simulations provide evidence for the existence of at least two stable states for magnesium binding to the hammerhead RNA. In one state, corresponding to the crystal at pH 5.0, a Mg^{2+} ion is bound at site 1 and there is a water molecule linking the *pro*-R_P anionic oxygen of the cleavable phosphate and a water of hydration of Mg^{2+} at site 1. In the second state, corresponding to the crystal at pH 8.5, two Mg^{2+} ions are bound close to the cleavable phosphate at sites 1 and 6 with an OH^- ion coordinated to both Mg^{2+} ions. The OH^- ion required for stabilizing the dimer of Mg^{2+} ions is bridging these cations similarly to the situation in μ-hydroxo complexes formed by olation of metal hydroxides (25,26). In line with the assumption of a μ-bridging OH^- is the observation that in X-ray analysis some density maps show continuous electron density between the metals at sites 1 and 6. The μ-hydroxo-bridged cluster is clearly superior to a single Mg^{2+} in stabilizing a high local concentration of OH^- in proximity of the active site and the activity of OH^- ions around the metal cluster may thus be higher.

Similar complexes of two metal ions bridged by OH^- were also proposed to be part of the active sites of binuclear metallohydrolases (27). For inorganic pyrophosphatase from *Escherichia coli*, experimental findings strongly suggest that an OH^- ion bridging two Mg^{2+} ions is involved in catalysis (28). Related situations are found in the crystal structures of mammalian phosphatase-1 and yeast enolase where two adjacent Mg^{2+} ions are bridged by a carboxylate oxygen (29,30). However, no calculations were performed on such systems. Interestingly, an anionic phosphate oxygen bridges two divalent metal ions at the 3′–5′ exonuclease active site of *Escherichia coli* DNA polymerase I where one metal ion is directly bound to another phosphate oxygen (31). It has been proposed that in the 3′–5′ exonuclease the bridged metal

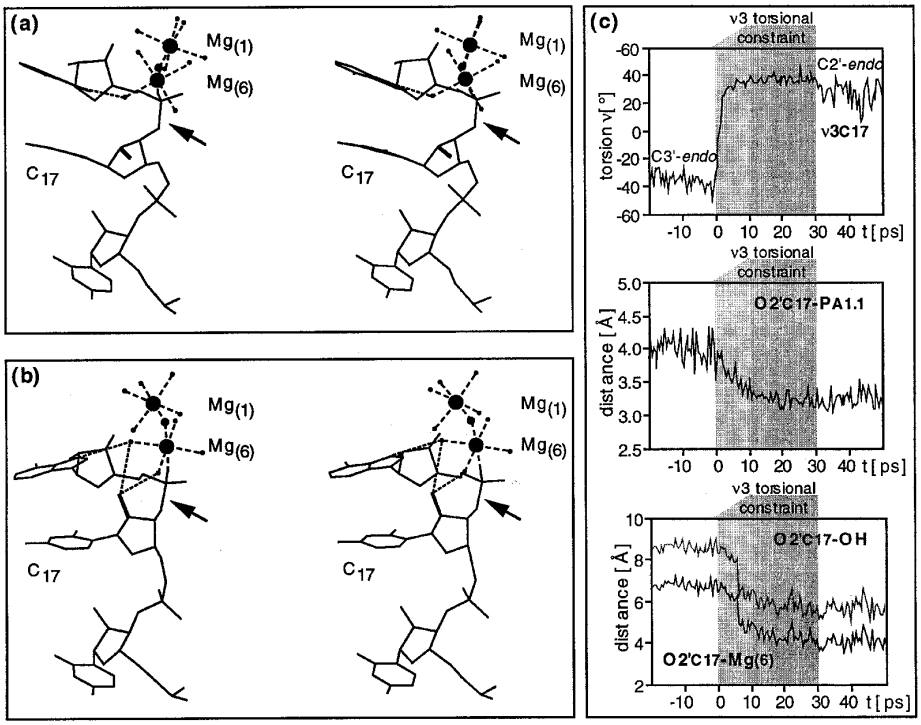

Figure 4. Stereoview showing the hammerhead active site with the Mg^{2+} ions at sites 6 and 1 along with the μ-bridging OH^- ion before **(a)** and after **(b)** the flip from C3′-*endo* to C2′-*endo* pucker at the C_{17} ribose. Distances within the range of hydrogen bonds between two water molecules bound to $Mg^{2+}{}_{(6)}$ and the 2′-hydroxyl group of C_{17} are indicated by dotted lines. The cleavable phosphodiester bond is indicated by an arrow. **(c)** A flip from C3′-*endo* to C2′-*endo* pucker of the C_{17} sugar was induced by forcing the ν3 ribose torsional angle (C2′-C3′-C4′-O4′) to values above 25° (shaded area). The starting structure for this simulation was a hammerhead conformation extracted after 430 ps of an unconstrained trajectory (Fig. 2). The torsional constraint was slowly switched on during the first 10 ps and released after 30 ps (top). In concert with the ribose flip the C_{17} 2′-hydroxyl moved closer than 3.5 Å to the attached phosphorous atom, to <6 Å from the μ-OH^- bridge, and to ~4 Å from $Mg^{2+}{}_{(6)}$ (middle and bottom panels and Fig. 3b). The conformational energy of the hammerhead RNA calculated from the AMBER force field (18) was not affected by the ribose flip.

cluster provides an OH^- ion necessary for catalysis (31). Subsequently, a general mechanism for DNA and RNA polymerases has been set up, where a complex of two Mg^{2+} ions bridged by an anionic phosphate oxygen stabilizes the transition state in the catalysis (32). X-ray structure analysis revealed this kind of geometry for two Mg^{2+} ions bridged by an anionic phosphate oxygen at the active site of rat DNA polymerase β (Fig. 3) (33). As in the *E.coli* inorganic pyrophosphatase, where fluoride ions are known to inhibit activity (34), probably by competition with an OH^- ion implicated in catalysis (28), the hammerhead ribozyme should be tested for activity in presence of F^- ions. In this respect, it is interesting to note that F^- ions also inhibit splicing in group I introns (35) which are also metalloenzymes (36) and for which the positions of two Mg^{2+} ions at the catalytic site have been proposed (37).

Could the bridging OH^- ion initiate hammerhead cleavage?

In the simulated MD trajectories, where the hammerhead conformations are always close to the crystal structure, the μ-hydroxo bridge was never seen in a favourable position for the direct activation of the cleavage-site 2′-hydroxyl. As such, this observation is not surprising since the conformational sampling is done around the equilibrium state, from which input of activation energy is required in order to reach the transition state. Simulations performed at higher temperatures up to 350 K followed by rapid cooling led at times to only slightly shorter distances between the 2′-hydroxyl oxygen atom and the cleavable phosphate (data not shown). However, when a flip of the ribose pucker from C3′-*endo* to C2′-*endo* at the C_{17} residue which holds the cleavable 3′-phosphate was induced during the simulations, the reactive-site 2′-hydroxyl moved in close proximity to both the attacked phosphorous atom and the μ-bridging OH^- ion (Fig. 4). At the same time, the 2′-hydroxyl comes within hydrogen bonding distance of two water molecules bound to the Mg^{2+} ion at site 6 (Fig. 4b). Although the present study does not show evidence for it, the sugar flip could constitute a conformational rate-limiting step. At room temperature, only a few hammerhead molecules could probably enter the thermally-driven conformational change from the inactive C_{17}-C3′-*endo* to the active C_{17}-C2′-*endo* pucker. This makes the pucker flip a rare process which is beyond the nanosecond time scale of the present MD simulations. It was speculated earlier that among other conformational changes such a flip of the C_{17} ribose pucker could be necessary for the hammerhead self-cleavage (9,38).

The Mg^{2+} ion at site 4 could also participate in the conformational change from ground state to the transition state. In the MD simulations, this ion dissociated from its site in the crystal structure in proximity to the base of G5, a nucleotide essential for catalysis (2). It might be possible that the release of the Mg^{2+} ion at site 4 is required for facilitating the conformational change. Interestingly, dissociation of Mg^{2+} ions from the hammerhead RNA upon cleavage is experimentally observed (39).

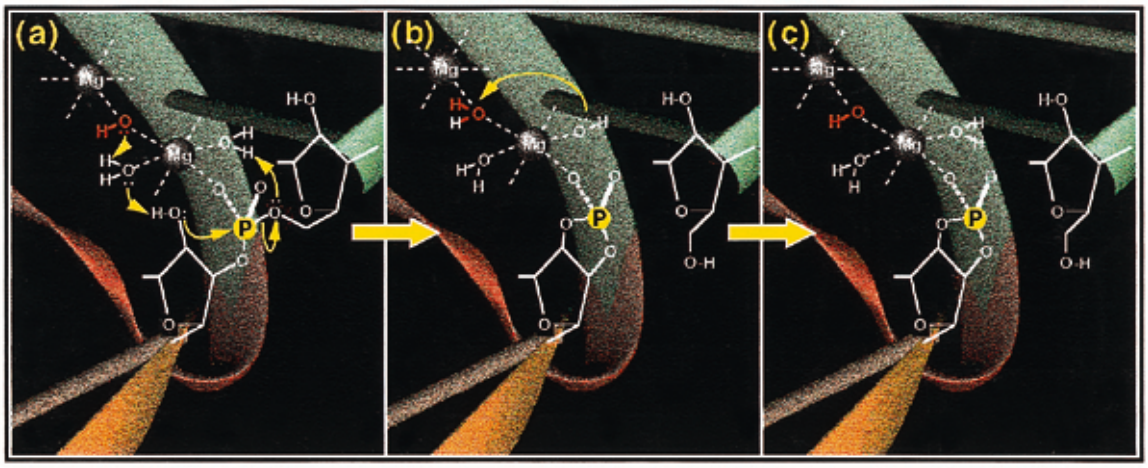

Figure 5. New mechanism for hammerhead ribozyme cleavage proposed on the basis of MD simulations of the crystal structure. **(a)** After trapping of an OH^- between two Mg^{2+} ions in the deep groove, a flip from C3′-*endo* to C2′-*endo* pucker at the C_{17} ribose moves the cleavage-site 2′-hydroxyl group in proximity to the hydration sphere of the $Mg^{2+}{}_{(6)}$ ion bound to the cleavable phosphate. The μ-bridging OH^- between $Mg^{2+}{}_{(1)}$ and $Mg^{2+}{}_{(6)}$ abstracts a proton from a metal-bound water molecule, which then activates the proximal 2′-hydroxyl group. The activated 2′-hydroxyl attacks the adjacent 3′-phosphate leading to the 2′3′-cyclic phosphate and 5′-hydroxyl products **(b)**. It is further suggested that the initial state is recovered by proton transfer from a metal-bound water molecule to the 5′-hydroxyl group of one product **(c)**. The fate of the μ-hydroxo-bridged magnesium cluster after cleavage is unknown. The outlines of this new detailed mechanism are consistent with the available structural data and the earlier proposed cleavage chemistry (4) where a metal-bound hydroxide activates the cleavage-site 2′-hydroxyl group (Fig. 1b and c).

After the change in sugar pucker from C3′-*endo* to C2′-*endo*, we speculate that proton shuffling could occur within the hydration sphere of the bound Mg^{2+} ions leading to proton abstraction from the 2′-hydroxyl and to proton donation to the 5′-hydroxyl of one cleavage product (Fig. 5) so that the final and initial states are identical, as expected for a catalytic mechanism. Within this proposed scheme, the same Mg^{2+} ion binds via water molecules to both the attacking and leaving oxygen groups. This proton shuffling mechanism does not arise from the simulations, although it is compatible with the distances and geometries within the simulated states. In the course of the proton shuffling mechanism, the μ-hydroxo bridge stores transiently a proton, a capacity facilitated by the lower basicity of hydroxide when coordinated to metal ions (40). The moderate basicity of the μ-OH^- ion might allow for a favourable equilibrium between both proton transfer steps, first in the deprotonation of a metal-bound water by the μ-OH^- ion and secondly in the final deprotonation of the μ-H_2O by an OH^- ion bound to the metal (Fig. 5).

Protonation of the bridging OH^- ion and the suggested ensuing proton shuffling are expected to have much shorter timescales than that of the present simulations, and the instability on the 10 picosecond timescale of the binuclear metal center with a bridging water molecule transiently formed during proton shuffling does not constitute a contradiction. The sluggish rate of the overall catalytic reaction (minute timescale) is probably related to activation energies linked to the trapping of the binuclear center and to the C3′-*endo* to C2′-*endo* conformational change.

CONCLUSIONS

The present simulations suggest that, during hammerhead ribozyme catalysis, the 2′-hydroxyl nucleophile which attacks the cleavable phosphate is activated from the deep groove side of stem I where Mg^{2+} ions 6 and 1 are located in the crystal structure (Fig. 1d). The two-metal-ion mechanism proposed here for hammerhead ribozyme cleavage is defined by the role of the μ-hydroxo-bridged Mg^{2+} cluster which provides the OH^- ion activating the 2′-hydroxyl nucleophile (Fig. 4a). A minimal conformational change in the RNA restricted to a single sugar pucker change from C3′-*endo* to C2′-*endo* is sufficient for initiating the cleavage (Fig. 4b).

ACKNOWLEDGEMENTS

W.G.S. thanks S. Lippard for useful discussions. We thank C. Massire for help with the DRAWNA program in preparation of Figure 1a and K. Taira for sending E.W. unpublished work. We are much indebted to Peter Kollman and his group at UCS F. for making available to us the latest version of the AMBER MD package used in the present study. T.H. is supported by an EMBO long-term fellowship.

REFERENCES

1 Uhlenbeck, O. (1987) *Nature*, **328**, 596–600.
2 McKay, D.B. (1996) *RNA*, **2**, 395–403.
3 Scott, W.G. and Klug, A. (1996) *Trends Biochem. Sci.*, **21**, 220–224.
4 Dahm, S.C., Derrick, W.B. and Uhlenbeck, O.C. (1993) *Biochemistry*, **32**, 13040–13045.
5 Thomson, J.B., Tuschl, T. and Eckstein, F. (1996) In Eckstein, F. and Lilley, D.M.J. (eds), *Catalytic RNA*, Springer, Berlin, pp. 173–196.
6 Scott, W.G., Murray, J.B., Arnold, J.R.P., Stoddard, B.L. and Klug, A. (1996) *Science*, **274**, 2065–2069.
7 Scott, W.G., Finch, J.T. and Klug, A. (1995) *Cell*, **81**, 991–1002.
8 Pley, H.W., Flaherty, K.M. and McKay, D.B. (1994) *Nature*, **372**, 68–74.
9 Setlik, R.F., Shibata, M., Sarma, R.H., Sarma, M.H., Kazim, A.L., Ornstein, R.L., Tomasi, T.B. and Rein, R.J. (1995) *Biomol. Struct. Dynam.*, **13**, 515–522.
10 Birikh, K.R., Heaton, P.A. and Eckstein, F. (1997) *Eur. J. Biochem.*, **245**, 1–16.
11 Zhou, D.M., Usman, N., Wincott, F.E., Matulic-Adamic, J., Orita, M., Zhang, L.H., Komiyama, M., Kumar, P.K.R. and Taira, K. (1996) *J. Am. Chem. Soc.*, **118**, 5862–5866.
12 Zhou, D.M., Kumar, P.K.R., Zhang, L.H. and Taira, K. (1996) *J. Am. Chem. Soc.*, **118**, 8969–8970.
13 Pontius, B.W., Lott, W.B. and von Hippel, P.H. (1997), *Proc. Natl. Acad. Sci. USA*, **94**, 2290–2294.

14 Allen, M.P. and Tildesley, D.J. (1987) *Computer Simulation of Liquids*. Clarendon, Oxford.
15 Auffinger, P. and Westhof, E. (1996) *Biophys. J.*, **71**, 940–954.
16 Auffinger, P., Louise-May, S. and Westhof, E. (1997) *Faraday Discuss.*, **103**, 151–174.
17 Pearlman, D.A., Case, D.A., Caldwell, J.W., Ross, W.S., Cheatham, T.E., DeBolt, S., Ferguson, D., Seibel, G., Singh, U.C., Weiner, P.K. and Kollman, P.A. (1994) AMBER 4.1, San Francisco.
18 Cornell, W.D., Cieplak, P., Bayly, C.I., Gould, I.R., Merz, K.M., Ferguson, D.M., Spellmeyer, D.C., Fox, T., Caldwell, J.W. and Kollman, P.A. (1995) *J. Am. Chem. Soc.*, **117**, 5179–5197.
19 Åqvist, J.J. (1990) *J. Phys. Chem.*, **94**, 8021–8024.
20 Lee, H., Darden, T.A. and Pedersen, L.G.(1995) *J. Chem. Phys.*, **102**, 3830–3834.
21 Berendsen, H.J.C., Grigera, J.R. and Straatsma, T.P. (1987) *J. Phys. Chem.*, **97**, 6269–6271.
22 Ryckaert, J.P., Ciccotti, G. and Berendsen, H.J.C. (1977) *J. Comput. Phys.*, **23**, 327–336.
23 Darden, T.A., York, D. and Pedersen, L.G. (1993) *J. Chem. Phys.*, **98**, 10089–10092.
24 Pullman, A., Pullman, B. and Lavery, R. (1983) In Pullman, B. and Jortner J. (eds), *Nucleic Acids: The Vectors of Life*, Reidel, Dordrecht, pp. 75–88.
25 Cotton, F.A. and Wilkinson, G. (1988) *Advanced Inorganic Chemistry*. Wiley, New York.
26 Gorun, S.M. and Lippard S.J. (1986) *Nature*, **319**, 666–668.
27 Wilcox, D.E. (1996) *Chem. Rev.*, **96**, 2435–2458.
28 Salminen, T., Käpylä, J., Heikinheimo, P., Kankare, J., Goldman, A., Heinonen, J., Baykov, A.A., Coopermann, B.S. and Lahti, R. (1995) *Biochemistry*, **34**, 782–791.
29 Goldberg, J., Huang, B., Kwon, Y., Greengard, P., Nairn, A. and Kuriyan, J. (1995) *Nature*, **376**, 745–753.
30 Larsen, T.M., Wedekind, J.E., Rayment, I. and Reed, G.H. (1996) *Biochemistry*, **35**, 4349–4358.
31 Beese, L.S. and Steitz, T.A. (1991) *EMBO J.*, **10**, 25–33.
32 Steitz, T.A. (1993) *Current Opin. Struct. Biol.*, **3**, 31–38.
33 Pelletier, H., Sawaya, M.R., Kumar, A., Wilson, S.H. and Kraut, J. (1994) *Science*, **264**, 1891–1903.
34 Baykov, A.A., Alexandrov, A.P. and Smirnova, I.N. (1992) *Arch. Biochem. Biophys.*, **294**, 238–243.
35 Partono, S. and Lewin, A.S. (1990) *Nucleic Acids Res.*, **19**, 605–609.
36 Cech, T. (1993). In Gesteland, R.F. and Atkins, J.F. (eds), *The RNA world*, Cold Spring Harbor Laboratory Press, New York, pp. 239–269.
37 Streicher, B., Westhof, E. and Schroeder, R. (1996) *EMBO J.*, **15**, 2556–2564.
38 Mei, H.Y., Kaaret, T.W. and Bruice, T.C. (1989) *Proc. Natl. Acad. Sci. USA*, **86**, 9727–9731.
39 Long, D.M., LaRiviere, F.J. and Uhlenbeck, O.C. (1995) *Biochemistry*, **34**, 14435–14440.
40 Baes, C.F. and Mesmer, R.E. (1976) *The Hydrolysis of Cations*. Wiley, New York.
41 Delarue, M., Poch, O., Tordo, N., Moras, D. and Argos, P. (1990) *Protein Engng.*, **3**, 461–467.
42 Sousa, R. (1996) *Trends Biochem. Sci.*, **21**, 186–190.